A series of cobalt bis(thiosemicarbazone) catalysts for effective photocatalytic hydrogen evolution reaction

Michael Papadakis, Georgios Landrou, Marie Poisson, Léa Delmotte, Katerina a G Achileos, Sylvain Bertaina, Renaud Hardré, Kalliopi Ladomenou, Athanassios G Coutsolelos, Maylis Orio

RESEARCH ARTICLE

A series of cobalt bis(thiosemicarbazone) catalysts for effective photocatalytic hydrogen evolution reaction

Michael Papadakis,[+[a]] Georgios Landrou,[+[b]] Marie Poisson,[[a]] Léa Delmotte,[[a]] Katerina Achileos,[[b]] Sylvain Bertaina,[[c]] Renaud Hardré,[[a]] Kalliopi Ladomenou,*[[d]] Athanassios G. Coutsolelos,*[[b,e]] and Maylis Orio*[[a]]

[a] Dr. M. Papadakis, M. Poisson, L. Delmotte, Dr. R. Hardré, Dr. M. Orio
Aix-Marseille Univ, CNRS, Centrale Marseille, iSm2, Marseille, France
E-mail: maylis.orio@univ-amu.fr, https://ism2.univ-amu.fr/fr/biosciences/biosciences
[b] Dr. G. Landrou, K. Achileos, Prof. A. G. Coutsolelos
University of Crete, Chemistry Department, Laboratory of Bioinorganic Chemistry, Heraklion, Greece.
E-mail: acoutsol@uoc.gr, http://www.chemistry.uoc.gr/coutsolelos/
[c] Dr. S. Bertaina
Aix-Marseille Univ, CNRS, IN2MP UMR 7334, Marseille, France
[d] Assist. Prof. Kalliopi Ladomenou
International Hellenic University, Department of Chemistry, Laboratory of Inorganic Chemistry, Agios Loucas, Kavala, Greece.
E-mail: kladomenou@chem.ihu.gr, https://kladomenou.wixsite.com/ladomenou
[e] Institute of Electronic Structure and Laser, Foundation for Research and Technology - Hellas, Vassilika Vouton, Heraklion, Greece.
+ Equal contribution

Supporting information for this article is given via a link at the end of the document.

Abstract: In order to diminish environmental issues such as global warming due to increased carbo dioxide (CO_2) emissions, considerable efforts have been made in the research community. Photocatalytic hydrogen (H_2) production is a very important way towards this goal, since sunlight is an abundant source of energy and H_2 is a clean fuel, producing no greenhouse gases. Inexpensive, stable and non-toxic carbon dots were easily synthesized and used as photosensitizers in water in the presence of a series of molecular cobalt catalysts (**CoTSC**). The catalysts were thiosemicarbazone-based complexes able to transfer electrons for hydrogen evolution reaction. Under visible light irradiation, the nitrogen-doped carbon dots (**NCdots**) transfer the photoexcited electrons to the catalyst, producing an activity of 358 µmol $g_{NCdot}^{-1}h^{-1}$ (TON_{Co}=570) for **CoTSC-N(CH$_3$)$_2$CN** after 24h of irradiation. These types of molecular catalysts display great activity and stability in combination with the easily synthesized and modified carbon dot materials.

Introduction

Global energy markets are under stress and oil prices have reached record levels. In some European countries, energy prices in 2021 were ten times higher than the 2020 average.[1] Moreover, the shortage of supplies across the European Union (EU) reinforces the need for less fossil fuels consumption and further use of alternative renewable energy sources.[2] This strategy will lead to energy security, since the use of renewable energy in industry, power generation and transport will lower prices overtime. Moreover, CO_2 emissions will be reduced in order to decrease global warming and attain a greener and more sustainable future. Among the renewable energy sources, hydrogen is seen as a promising choice, as it produces zero pollutants upon its subsequent combustion.[3] A promising way to produce hydrogen is the photochemical evolution process, inspired by natural photosynthesis. During this procedure, a photosensitizer absorbs light efficiently, a catalyst mediates the reduction of protons into hydrogen and a sacrificial electron donor (SED) regenerates the whole process by providing electrons to close the cycle.[4] Inspired by Nature's hydrogenase enzymes, which contain inorganic cofactors that mediate the reversible conversion of protons and electrons into hydrogen, a large number of biomimetic and bio-inspired catalysts have emerged in the past years.[5] Earth-abundant molecular catalysts with an active metal site and specific ligands are able to tune the coordination environment for efficient H_2-evolution. The currently most efficient molecular catalysts for H_2-evolution are based on first-row transition metal ions like cobalt or nickel.[6-18] Moreover, thiosemicarbazone based ligands have been examined as a new class of electro- and photocatalysts.[19-24] This type of catalysts are proved to be efficient with low overpotential requirements and the ligands are able to store and transfer electrons and protons for the hydrogen evolution reaction (HER). On the other hand, a suitable photosensitizer is essential to absorb light, to transfer electrons and to enhance photostability. Carbon dots (**Cdots**) possess all the required features and have been efficiently used by our group and others for HER. In a recent study, the photocatalytic capabilities for hydrogen production of a series of mononuclear thiosemicarbazone nickel complexes as catalytic centers and nitrogen-dopped carbon dots (**NCdots**) as light-harvesting materials were evaluated.[20] The thiosemicarbazone nickel complexes considered in this work were prepared with redox active ligands possessing different electronic properties. We could probe the most efficient photocatalytic system as being the **NCdots** associated with the dimethylamino-thiosemicarbazone nickel catalyst, **NiTSC-N(CH$_3$)$_2$**, with a calculated Turn-Over Number (TON) of 148 when using a TCEP/Asc (1:1) mixture as SED, at pH=5 and under white led radiation for 30h in water. While the chemical nature of the substituent in the para position of the ligand was shown to influence the photocatalytic behavior of the systems and their hydrogen evolution performances, no clear rational could be

drawn when looking at the catalysis parameters and the electronic properties of the ligands.

To further explore such correlation, we envisioned a possible effect of the metal from the catalytic centers, based on previous reports showing that switching from nickel to cobalt positively affects the overpotential requirement and changes the reaction mechanism for electrocatalytic HER.[25] Therefore, carbon dots photosensitizers and a series of thiosemicarbazone cobalt complexes were prepared and investigated towards photocatalytic hydrogen evolution. More specifically, we report the synthesis of molecular cobalt-based catalysts having different chemical substituents in para position of the phenyl ring, thus providing different electron-donating/accepting features to the thiosemicarbazone ligands. The following series was considered in our study: **CoTSC-OCH$_3$**, **CoTSC-CN**, **CoTSC-N(CH$_3$)$_2$**, and **CoTSC-N(CH$_3$)$_2$CN** (Figure 1). As photosensitizers, carbon dots (**Cdots**) and nitrogen-doped carbon dots (**NCdots**) were used as they feature several advantages such as ease and low-cost preparation as well as good efficiency towards light absorbance and electron transfer. In this work, we evaluated the capabilities of the new photocatalytic systems to promote hydrogen evolution in aqueous solution, in the presence of a sacrificial electron-donor and under visible light irradiation. Mechanistic investigations based on fluorescence studies were performed with the aim to elucidate the reaction pathway of our systems in the presence of carbon dots using different concentration of cobalt catalysts. Our results show great promise for the new cobalt-containing systems that outperform the previously reported nickel-based photocatalysts in the context of photo-induced hydrogen production.

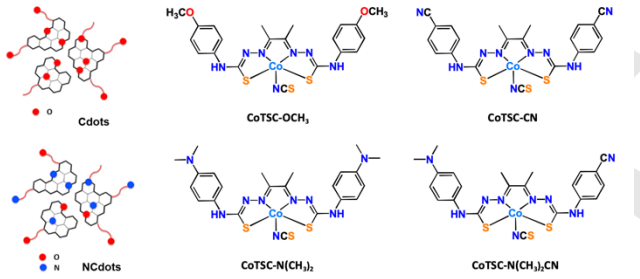

Figure 1. Chemical structures of photosensitizers and molecular catalysts.

Results and Discussion

Synthesis and characterization of cobalt catalysts

Our group reported the synthesis and characterization of a cobalt catalyst (**CoTSC-OCH$_3$**, Figure 1) that exhibited electrocatalytic activity for proton reduction to dihydrogen with a low overpotential requirement.[25] Based on these encouraging results and our recent photocatalytic study on nickel analogs combined with noble metal-free photosensitizers, we wish to examine the capability of cobalt catalysts towards photochemical hydrogen evolution. Following previously reported protocols,[21] we synthetized a series of symmetric ligands using three different substituents such as methoxy (-OCH$_3$), dimethylamino (-N(CH$_3$)$_2$) and cyano (-CN) groups and we also prepared an asymmetric ligand combining dimethylamino and cyano groups (-N(CH$_3$)$_2$, CN). The cobalt complexes were obtained in moderate yields (from 26 to 53%) by adding 1.5 equivalent of Co(NCS)$_2$ to a suspension of one equivalent ligand in methanol. The crude compounds precipitated as solid powders after washing with cold water and methanol and were further purified on neutral alumina liquid chromatography columns. The sets of complexes were characterized by HRMS ESI, NMR and FT-IR spectroscopies (see Supporting Information).

To address the question of the spin configuration of the cobalt ion, the magnetic properties of the complexes were investigated in the solid state using the SQUID technique. Figure 2 shows the dependence of the magnetic susceptibility on the temperature, χ.T (blue lines) for the series of complexes. Considering the solid-state structure of the **CoTSC-OCH$_3$** catalyst previously reported as a dimer,[25] all complexes were treated as dinuclear species. The green line represents the best fit for a paramagnetic system S = 3/2 having one low-spin Co^{III} center (S=0) and one high-spin Co^{II} center (S = 3/2). In this case, χT is 1.875 cm^3.K.mol^{-1} and is temperature independent. The orange line represents the best fit for a diamagnetic system S=0 having two low-spin Co^{III} centers (S=0). All complexes present a similar behavior with the magnetic susceptibility curves being consistent with the presence of the cobalt ions being diamagnetic low-spin Co^{III} centers. The deviation of the curves from the best fit for a diamagnetic system (orange line) is attributed to contamination from paramagnetic high-spin Co^{II}. This contribution was estimated to be of 9%, 4%, < 1%, and 8.5% for **CoTSC-N(CH$_3$)$_2$CN**, **CoTSC-OCH$_3$**, **CoTSC-CN** and **CoTSC-N(CH$_3$)$_2$**, respectively. These results are thus in agreement with the data previously reported for **CoTSC-OCH$_3$** which was found to be a diamagnetic Co^{III} dimer.

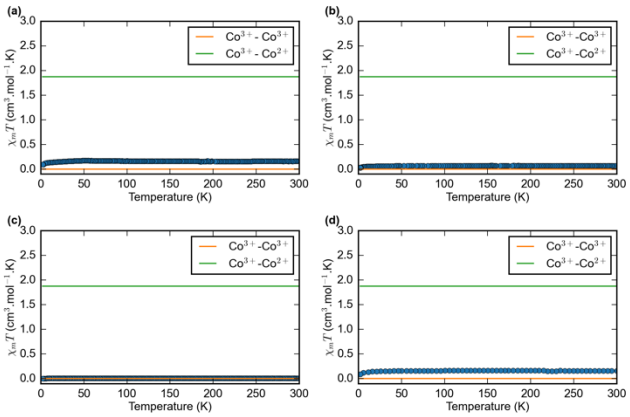

Figure 2. Temperature dependence of the magnetic susceptibility for a) **CoTSC-N(CH$_3$)$_2$CN**, b) **CoTSC-OCH$_3$**, c) **CoTSC-CN**, and d) **CoTSC-N(CH$_3$)$_2$**.

The solution properties of the complexes in DMF were investigated by ESI-MS, NMR, and FT-IR spectroscopic techniques. Consistently with our previous study on **CoTSC-OCH$_3$**, these data show that the complexes are diamagnetic having a singlet S=0 ground spin state. They also indicate the presence of monomers having low spin Co(III) centers bound to an axial NCS anion and a DMF molecule. These latter features are further supported by DFT computations that enabled us to assign the NCS$^-$ and DMF-based vibrational modes proving thus their coordination to the metal centre (see Supplementary Information, Table S1 and Figures S1-S3).

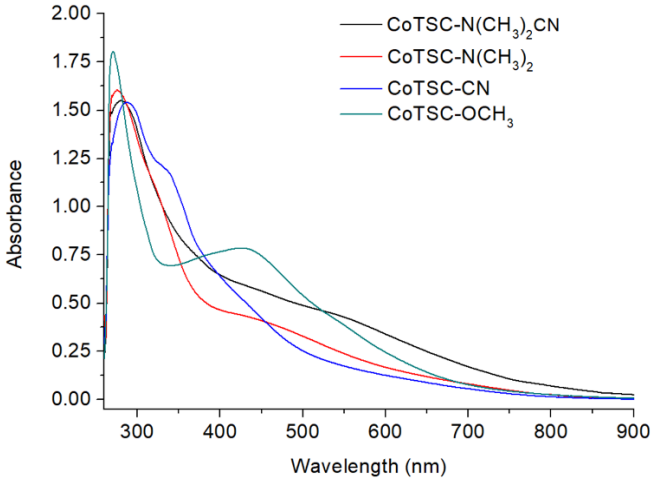

Figure 3. UV-vis spectra of a 0.05 mM solutions of the series of **CoTSC** complexes in DMF.

UV-vis spectra of the complexes were recorded to examine the electronic properties of the complexes. The UV-vis spectra display a main absorption band ranging between 336 and 550 nm (Table S2). There is also a second absorption band detected for all complexes between 271 to 287 nm which is reminiscent of the ligand. Interestingly, the **CoTSC-N(CH$_3$)$_2$CN** complex bears two shoulder-like absorptions at 449 and 550 nm, due to its asymmetrical nature that affects the electron density distribution within the ligand as observed in the case of the nickel analogues (Figure 3). Overall, the spectral features of the cobalt complexes are similar to those from the nickel series and the observed shifts of the main absorption band are also attributed to the different electronic donating properties of the phenyl ring substituents.
The redox behaviors of the complexes were investigated by cyclic voltammetry (CV) at room temperature using a glassy carbon electrode in anhydrous DMF with 0.1m TBAPF$_6$ as the supporting electrolyte (Figure S4).

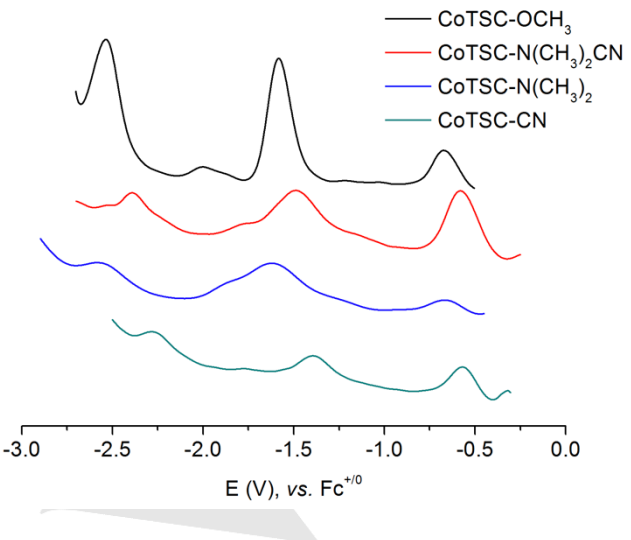

Figure 4. Differential pulse voltammetry curves for the series of **CoTSC** complexes in DMF.

In the cathodic region, the cyclic voltammograms of the complexes display three redox systems: two quasi-reversible are observed between -0.54 and -0.67, and between -1.33 and -1.62 V vs. $Fc^{+/0}$ while the irreversible ones occur between -2.23 and -2.58 V vs. $Fc^{+/0}$ (Figure 4 and Table 1).

Table 1. Electrochemical data for the **CoTSC** series of complexes. Potentials (V) refer to $Fc^{+/0}$.

Complex	$[Co^{III}]/[Co^{II}]^-$	$[Co^{II}]^-/[Co^{II}\text{-}L^{\cdot}]^{2-}$	$[Co^{II}\text{-}L^{\cdot}]^-/[Co^{I}\text{-}L^{\cdot}]^{3-}$
CoTSC-N(CH$_3$)$_2$CN	-0.57	-1.48	-2.39
CoTSC-OCH$_3$	-0.65	-1.58	-2.53
CoTSC-CN	-0.54	-1.33	-2.23
CoTSC-N(CH$_3$)$_2$	-0.67	-1.62	-2.58

The redox behavior of the complexes in the cathodic region being similar to that of **CoTSC-OCH$_3$**, the reduction events can be ascribed as successive metal-based, ligand-based and metal-based processes producing the Co(II), Co(II)-ligand radical and Co(I)-ligand radical species. In our previous work, we proposed that we start with an octahedral low-spin (S=0) Co(III) complex bound to both NCS and DMF ligands. The first reduction process occurs upon dissociation of the DMF molecule and yields a pentacoordinated Co(II) species in the doublet state. The second reduction process occurs upon dissociation of the NCS^- ligand and yields an open-shell singlet resulting from the interaction between the Co(II) centre and the thiosemicarbazone-based radical. Finally, the third reduction occurs at the metal centre to produce the Co(I) species interacting with the radical species and yields a doublet state.[24] Such a rationale has been further investigated using DFT computations to predict the redox potentials of the series of complexes. The good agreement between calculated and experimental values confirms the proposed electronic structures of the species formed upon successive reduction and thus support the above assignments (Tables S3-S6).

Photocatalytic H_2 evolution studies.

As a follow-up to our previous investigations on the nickel complexes, we studied the new family of cobalt catalysts under similar conditions. We prepared aqueous solutions containing a 1:1 ratio of TCEP/Asc as SED at pH=5. Carbon dots (**Cdots**) were first tested as photosensitizers and combined with the cobalt complexes as catalytic centers but none of the resulting photocatalytic systems led to significant hydrogen production upon white led irradiation. In addition, we showed that **Cdots** were unable to produce hydrogen when the thiosemicarbazone nickel complexes were used as molecular catalysts. It was suggested that **CDots** could not absorb visible light, since it has been reported that they are able to evolve H_2 with TON_{Co}=64 after 23h under UV light irradiation in the presence of a cobalt molecular catalyst (CatCo(III)1).[19] Moreover, when comparing the photocatalytic ability of **Cdots** and **NCdots** in similar experimental conditions, under UV irradiation and in the presence of CatCo(III)1, **NCdots** were proved to be more efficient towards H_2 evolution.

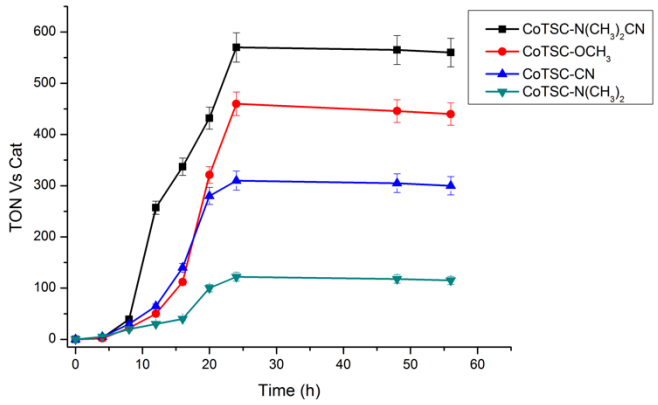

Figure 5. Photocatalytic hydrogen production plots of 10 mg **NCdots** with 150 nmol cobalt catalysts: **CoTSC-N(CH$_3$)$_2$CN**, **CoTSC-OCH$_3$**, **CoTSC-CN** and **CoTSC-N(CH$_3$)$_2$**. All photocatalytic experiments were performed in aqueous solution of TCEP/Asc (1:1) 0.1 M each at pH = 5. All reported values result from an average of three independent measurements.

This is likely due to the presence of nitrogen-containing doped atoms inside the aromatic domains that enhance the absorption of the material at 340 nm with a long tail reaching around 470 nm. Consequently, hydrogen production was detected upon photo-irradiation in the visible region with all prepared cobalt catalysts when **NCdots** were used. All experiments were performed under the same experimental conditions (Figure 5).

To determine the optimum quantity of complex to be used in the new photocatalytic system, we used five different concentrations to prepare our samples. For solutions containing 20 nmol of complex, no photo-evolved H_2 was detected. When we increased the quantity of catalyst to 50 nmol, an adequate amount of hydrogen was produced in these conditions. We further increased the catalyst quantity to 100 nmol which drastically improved the turnover number value *versus* the catalyst, (TON_{Co}=565). Successive increase in catalyst quantity to 150 nmol (TON_{Co}=570) and 200 nmol (TON_{Co}=562) did not further improve the total TON_{Co} values (Figure 6). For these reasons, the following photocatalytic experiments were performed using 100 nmol of each cobalt complex. In contrast to nickel complexes the maximum performance was obtained when 50 nmol of catalyst was used (see Supplementary Information).

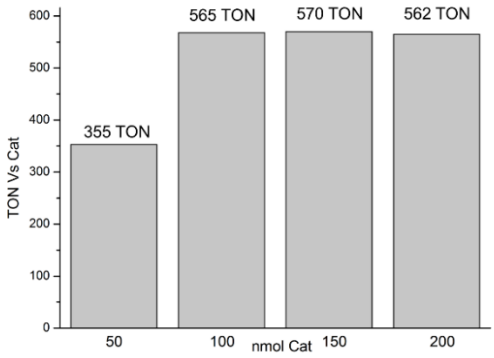

Figure 6. Photocatalytic hydrogen production plots of 10 mg **NCdots** with different amounts (50-200 nmol) of **CoTSC-N(CH$_3$)$_2$CN** catalyst. The photocatalytic experiments were conducted in aqueous solution of TCEP/Asc (1:1) 0.1 M each at pH = 5. All reported values result from an average of three independent measurements (within 5-10% error).

For the cobalt series, the best catalyst of the group was found to be the asymmetrical complex bearing dimethylamino and cyano groups, **CoTSC-N(CH$_3$)$_2$CN** (Figure 5). The system reached a plateau at about 24 hours, in a faster manner compared to the average 30 hours needed for the nickel series. The results of the optimized photocatalytic experiments using all cobalt complexes are given in Figure 7 and Table 2. The best noble metal-free photocatalytic system contained 10 mg of **NCdots**, 0.1 M of TCEP/Asc in a 1:1 ratio and 150 nmol of **CoTSC-N(CH$_3$)$_2$CN** in an aqueous solution at pH=5 under white led irradiation. The **CoTSC-N(CH$_3$)$_2$CN** catalyst exhibited the highest stability (TON_{Co}=570) and the best total H_2 evolution efficiency of 358 µmol g_{NCdot}^{-1} h^{-1}. This performance is one of the best existing in the literature for this kind of systems. The H_2 production of **CoTSC-N(CH$_3$)$_2$CN** is about 8 times greater compared to our previous work with a CatCo(III)1 molecular catalyst (86 µmol vs 11.6 µmol).[19] Looking at the TON_{Co} values, the relative photocatalytic activity of the cobalt series is the following: **CoTSC-N(CH$_3$)$_2$CN** > **CoTSC-OCH$_3$** > **CoTSC-CN** > **CoTSC-N(CH$_3$)$_2$**. These H_2-evolution data show that the results for the three substituents are in agreement with their electron donating ability in the para position (-N(CH$_3$)$_2$ > -OCH$_3$ > -CN). The **CoTSC-N(CH$_3$)$_2$** catalyst does not follow this trend since it exhibits the lowest H_2 production performance while having the highest electron-donating ability. This is in line with the observations on the nickel catalysts studied in our previous work where no correlation between the photocatalytic performances and the electronic properties of the ligands could be drawn. Moreover, the **NiTSC-N(CH$_3$)$_2$** catalyst had the greatest performance with TON_{Ni}=148 whereas its Co counterpart shows the lowest H_2 production efficiency with TON_{Co}=122. Therefore, it seems, once again, that the chemical nature of the ligands does affect the hydrogen evolution performance of the system in a rational manner. Focusing on the ligand nature, the cobalt series performs in the same way as the nickel family but displays increased hydrogen production with exception of the dimethylamino-containing ligand. When comparing the two series, it becomes obvious that the cobalt series greatly improved the catalytic performances with respect to the nickel series. The complexes with asymmetrical and methoxy substituents display catalytic performances 8 times larger when transitioning from a nickel center to a cobalt one, whereas the performances of the cyano one is about 6 times larger.

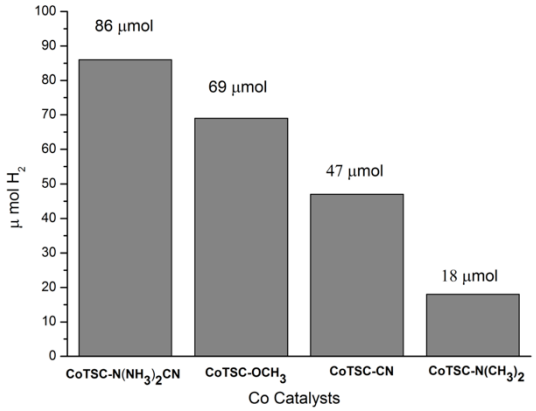

Figure 7. Photocatalytic hydrogen production (µmol H_2) upon irradiation of 10 mg **NCdots** in the presence of 150 nmol of cobalt catalysts in aqueous TCEP/Asc (1:1) 0.1 M each at pH = 5. All reported values result from an average of three independent measurements (within 5-10% error).

Table 2. Summary of the best photocatalytic data collected for each cobalt catalyst.

	TON_{Co} [a]	H_2 evolution rate $\mu mol\ g_{NCdot}^{-1}\ h^{-1}$) [b]
CoTSC-N(CH$_3$)$_2$CN	570	358
CoTSC-OCH$_3$	460	288
CoTSC-CN	310	196
CoTSC-N(CH$_3$)$_2$	122	75

[a] TON in 24 hours *vs.* catalyst [b] H_2 evolution rate ($\mu mol\ g_{NCdot}^{-1}\ h^{-1}$) *vs.* total g of NCdot in 24 hours.

As for the nickel complexes, we also performed control experiments with the cobalt series. Mercury was introduced in the system to provide proof that the observed catalysis is due to the molecular complexes and does not result from the formation of any nanoparticles. Upon the addition of a few Hg drops, no change in hydrogen production was observed. Additional experiments were performed in the absence of either catalyst, photosensitizer, SED or light irradiation. When **NCDot** and SED were used under irradiation, a negligible amount of H_2 was detected while in all other cases, no H_2 was produced. Lastly, replacing the cobalt complexes with $Co(NCS)_2$, a negligible amount of 4.2 µmol H_2 was produced. Finally, regeneration experiments were performed once the system reached a plateau. To our best system, addition of 10 mg of **NCdot** was enough to restart the H_2 production, proving the high stability and great performance of the catalyst. This is in accordance with another study where a molecular nickel catalyst proved to be stable under visible light irradiation.[26]

Photocatalytic mechanism. The thermodynamic ability for photochemical hydrogen evolution was evaluated by measuring the redox potentials of all nickel catalysts and the **NCdot** photosensitizer (Table 3). We used the previously reported values for valence band (VB) and the conduction band (CB) of nitrogen-doped carbon dots.[27] Combining these data with the redox potentials of the cobalt catalysts described in the preceding section, we could calculated the ΔG (PS/Cat) for all the catalysts. All computed potentials result in negative values which nicely explain the photocatalytic activity of the cobalt catalysts and also rationalize the trend observed within the series with exception of the **CoTSC-CN** being not the most efficient system while having the highest ΔG(PS/Cat) values. It is obvious that hydrogen production is thermodynamically allowed for all the catalysts used in these photocatalytic systems.

To shed light on the mechanism of the photocatalytic system, fluorescence spectroscopy was used (Figures S5-S8). Specifically, emission spectroscopy experiments were carried out with a fixed quantity of photosensitizers using water as solvent and in the presence of various concentrations of cobalt catalysts. The series of catalysts were dissolved in a concentrated DMSO solution and various amounts of catalysts were further added, including the concentration used for the photocatalytic experiments. The emission spectra were monitored upon excitation at 340 nm and in all cases, the emission intensity significantly decreased with quenching values up to more than 90 %.

Table 3. Redox potentials (V *vs.* NHE) of the metal-free photosensitizer and cobalt catalysts with the thermodynamic driving forces of electron transfer processes ΔG_1 (PS/Cat) and ΔG_2 (PS/Cat) (eV).

Compounds	E_{VB} [a]	E_{CB} [b]	E_{00} [c]	
NCdot	1.01	-2.13	3.14	
	$E_{1/2,1}$ [d]	$E_{1/2,2}$ [d]	ΔG_1 (PS/Cat)	ΔG_2 (PS/Cat)
CoTSC-N(CH$_3$)$_2$CN	+0.06	-0.85	-2.19	-1.28
CoTSC-OCH$_3$	-0.02	-0.95	-2.11	-1.18
CoTSC-CN	+0.09	-0.70	-2.22	-1.43
CoTSC-N(CH$_3$)$_2$	-0.04	-0.99	-2.09	-1.14

[a] Oxidation potential measured by cyclic voltammetry referenced *vs.* NHE. [b] Values calculated as the difference between the oxidation potentials and the optical band gap energy E_{00} (eV). [c] E_{00} values calculated from the intersection between the normalized absorption and emission spectra. [d] Reduction potentials measured by cyclic voltammetry and referenced to NHE.

In addition, we calculated the Stern-Volmer (K_{SV}) and quenching constants based on Stern-Volmer plots (Table 4 and Figures S9-12), using the equation $I_o/I = 1 + K_{SV}[Q]$, where I_o and I are the fluorescence intensities observed in the absence and in the presence of each quencher, respectively, and [Q] is defined as the quencher concentration.[28] In agreement with previous reports, the K_{SV} constants were all found higher in the case of the catalysts compared to that of the SED (K_{sv} = 13.8). For all catalysts, the quenching constants ($K_Q = 7.1 \times 10^{12} – 14.6 \times 10^{12}$) are also found to be higher when compared to that of the SED ($K_Q = 1.3 \times 10^9$). The quenching is thus more important in the case of ascorbic acid under our photocatalytic experimental conditions since the SED concentration (0.1 M) is much higher compared to that of the catalyst (50×10^{-6} M). These data thus indicate that the first step of the reaction mechanism is the transfer of the photoinduced electron from the sacrificial electron donor to the carbon dots by reductive quenching.

Table 4. Stern-Volmer constant K_{sv} and quenching constant K_Q for the series of cobalt catalysts.

	K_{sv} (M^{-1})	$K_Q=K_{sv}/\tau$ ($M^{-1}s^{-1}$)
CoTSC-N(CH$_3$)$_2$CN	72207	7.2×10^{12}
CoTSC-OCH$_3$	71934	7.1×10^{12}
CoTSC-CN	146735	14.6×10^{12}
CoTSC-N(CH$_3$)$_2$	71268	7.1×10^{12}
Asc	13.8	1.3×10^9

Gathering all these experimental data allowed us to propose a reaction mechanism for photocatalytic H_2-evolution with the series of **CoTSC** complexes using **NCdots** photosensitizers (Scheme 1). Upon photoexcitation of nitrogen-dopped carbon dots under visible light irradiation, the electrons are transferred from the valence band (VB) to the conduction band (CB). This process leads to the creation of an electron hole in the photosensitizer VB that is compensated by an electron from the SED via a reductive

quenching process. The photogenerated electrons are then transferred to cobalt catalysts and used for HER in presence of a proton source. A series of chemical and electrochemical steps leads to formation and release of H_2 following a metal-centred pathway assisted by the redox-active TSC ligand.[29]

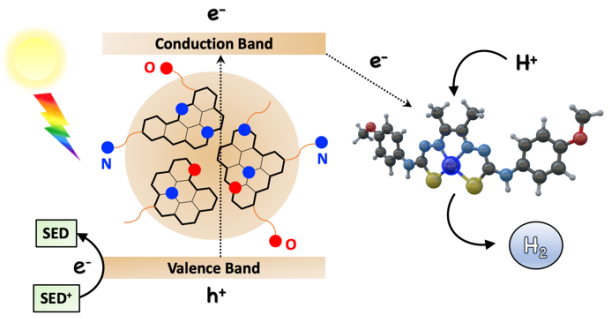

Scheme 1. Proposed reaction mechanism for photocatalytic H_2 evolution using Co complexes as catalytic centers and nitrogen-doped carbon dots as photosensitizer, with TCEP/Asc acting as sacrificial electron donor.

Conclusions

In this study a photocatalytic system comprised of water-soluble carbon dots (**NCdots**) used as photosensitizer and a series of Earth-abundant cobalt complexes used as catalysts (**CoTSC**), was able to produce hydrogen under light irradiation in water. The series of cobalt catalysts were successfully synthesized and characterized indicating that all monomers possess low spin Co(III) centres bound to an axial NCS anion and a DMF molecule. Also, DFT calculations are in perfect agreement with the experimental measurements suggesting the presence of axial ligands and helped identify the nature of species formed upon successive reductions. Symmetric and asymmetric complexes with different ligand substituents having different electron-donating properties were considered in this work. Our results demonstrated that all cobalt catalysts were able to produce H_2 under visible light irradiation in the presence of 0.1 M TCEP/Asc as sacrificial electron donor at pH=5. The system was optimized and the maximum activity with respect to **NCdot** was 358 μmol g_{NCdot}^{-1} h^{-1} (TON_{Co}=570) for **CoTSC-N(CH$_3$)$_2$CN**. A correlation between the activity of the catalysts and their electron donating ability could not be drawn. The system reached a plateau after 24h and could further produce H_2 upon the addition of fresh photocatalyst. The photocatalytic hydrogen evolution was performed via a reductive quenching by the SED. All cobalt catalysts showed enhanced H_2 production, from 6 to 9 times higher compared to the nickel counterparts we reported in our previous study, proving thus cobalt being superior in this type of molecular catalysts. Thiosemicarbazone cobalt catalysts in combination with carbon dot materials as photosensitizer were shown herein to have one of the best hydrogen production activity and stability under the experimental conditions. Opposed to most molecular catalysts having low stability, these cobalt catalysts are proven to be quite effective and are promising for further use in future studies employing additional photosensitizers.

Experimental Section

General. All reagents and solvents were purchased from usual commercial sources and used without further purification, unless otherwise stated. The synthesis and characterization of **NCdots** were reported in detail in our previous work.[27] The **CoTSC-OCH$_3$** complex was prepared according to the procedure previously described.[14, 30] Synthesis and characterization of the newly reported complex **CoTSC-N(CH$_3$)$_2$CN**, **CoTSC-CN** and **CoTSC-N(CH$_3$)$_2$** are described in the Supplementary Information. ^{1}H NMR spectra were recorded on Bruker 400 MHz Avance III Nanobay. Chemical shifts for ^{1}H NMR spectra are referred to TMS or the residual protonated solvent. IR spectra were re- corded with Bruker TENSOR27 spectrometer equipped with a single-reflection DuraSampIIR diamond. High resolution mass spectra (HRMS) were performed on a QStar Elite (Applied Biosystems SCIEX) spectrometer equipped with atmospheric pressure ionization source (API) pneumatically assisted. The samples were placed in a methanol/3 mM ammonium acetate. The results were validated by three measurements. UV/vis spectra were recorded on a Varian Cary 60 spectrophotometer.

Electrochemistry. Cyclic voltammetry experiments were performed using a Origaflex OGF01A potentiostat and a three-electrode setup consisting of a glassy carbon working electrode, a platinum wire counter electrode, and an $Fc^{+/0}$ reference electrode. Ferrocene was used as an internal standard with $E^0(Fc^{+/0})$ = 0.52V versus Ag/AgCl for each measurement. All studies were performed in deoxygenated DMF containing NBu_4PF_6 (0.1 M) as supporting electrolyte.

SQUID Magnetometry. Magnetic characterization has been performed using a conventional SQUID magnetometer MPMS-XL from Quantum Design working at a magnetic field up to 5 T and temperature down to 2 K. The samples (powder) are filled in polypropylene sleeves then sealed in order to remove the maximum of dioxygen, which give the signal around 50 K (antiferromagnetic transition). Diamagnetic contribution of the sample holder was removed as well as the diamagnetism of the series of complexes. Temperature dependence of the susceptibility was recorded at a constant magnetic field of 1T from room temperature to 2K.

DFT calculations. All calculations were performed using ORCA 5.0.4[31-32] with the BP86 functional[33-35] and the def2-TZVP(-f) basis set.[36] Full geometry optimizations were undertaken by taking advantage of the resolution of the identity (RI) approximation in the Split-RI-J variant[37] with the appropriate Coulomb fitting sets.[38] Increased integration grids (DefGrid2 in ORCA convention) and tight SCF convergence criteria were used. For according to the experimental conditions, these calculations were performed in DMF solvent by invoking the Control of the Conductor-like Polarizable Continuum Model (CPCM).[39] We considered various possible spin configurations, including open-shell singlets. For the latter, we performed Broken-Symmetry DFT calculations, using the "FlipSpin" feature of ORCA.[40-42] Free energies as well as normal mode vibrations were extracted from numerical frequencies calculations. All the calculated reduction potentials are relative to $Fc^{+/0}$. The calculated Gibbs free energy difference using the BP86 functional to account for ferrocene in DMF is ΔG = 4.92 eV.

Photophysical Measurements. The UV-Vis absorption spectra of all compounds in solution were obtained using a Shimadzu UV-1700 spectrophotometer in quartz cuvettes of 1 cm path-length. The emission spectra of all derivatives in solution were measured on a JASCO FP-6500 fluorescence spectrophotometer equipped with a red-sensitive WRE-343 photomultiplier tube (wavelength range: 200-850 nm).

Photocatalytic H_2 Evolution Experiments. The photocatalytic reactions were performed using TCEP and Asc as reversible sacrificial electron donors. In all experiments, 3 ml aqueous solution of TCEP/Asc (1:1) 0.1 M each at pH 5.0 and 10 mg of NCDot photosensitizer were used. The appropriate amount of catalyst was added in the reaction vessel from a stock solution of each Co catalyst dissolved in DMSO solvent. A 10 ml

flask was used with a rubber septum where the mixture was purged with nitrogen for 15 min in order to remove oxygen. The reaction mixture was continuously stirred with irradiated with a 100 W white led emitting lamp. At fixed time intervals, 100 µl were removed from the headspace of the flask and analyzed by Shimadzu GC 2010 plus chromatograph with a TCD detector and a molecular sieve 5 Å column (30 m - 0.53 mm) in order to measure the amount of H_2 evolved. The latter was then quantified using a calibration curve. The reported H_2 production and the Turn Over Number (TON) are all presented as an average of three independent experiments.

Acknowledgements

This research was funded by the General Secretariat for Research and Technology (GSRT) and Hellenic Foundation for Research and Innovation (HFRI; project code: 508). This research has been co-financed by the European Union and Greek national funds through the Regional Operational Program "Crete 2014-2020," project code OPS:5029187. Moreover, the European Commission's Seventh Framework Program (FP7/2007-2013) under grant agreement no. 229927 (FP7-REGPOT-2008-1, Project BIO-SOLENUTI) and the Special Research Account of the University of Crete are gratefully acknowledged for the financial support. The authors gratefully acknowledge financial support of this work by the French National Research Agency (ANR-19-CE05_0030_01).

Keywords: cobalt catalyst • carbon dots • photocatalysis • hydrogen evolution reaction • solar energy

[1] D. Raimi , E. Campbell , R. G. Newell, B. C. Prest, S. Villanueva, J. Wingenroth, in *Resources for the Future*, https://www.rff.org/publications/reports/global-energy-outlook-2022/, **2022**.
[2] EUR-Lex, in *https://eur-lex.europa.eu/legal-content/EN/TXT/?uri=CELEX%3A52022DC0643&qid=1669913060946#footnote144*, European Union, **2022**.
[3] S. Chakraborty, S. K. Dash, R. M. Elavarasan, A. Kaur, D. Elangovan, S. T. Meraj, P. Kasinathan, Z. Said, *Front. Energy Res.* **2022**, *10*.
[4] E. Nikoloudakis, I. López-Duarte, G. Charalambidis, K. Ladomenou, M. Ince, A. G. Coutsolelos, *Chem. Soc. Rev.* **2022**, *51*, 6965-7045.
[5] M. Orio, D. A. Pantazis, *Chem. Commun.* **2021**, *57*, 3952-3974.
[6] V. Artero, J.-M. Saveant, *Energy Environ. Sci.* **2014**, *7*, 3808-3814.
[7] J. L. Dempsey, J. R. Winkler, H. B. Gray, *J. Am. Chem. Soc.* **2010**, *132*, 16774-16776.
[8] J. L. Dempsey, B. S. Brunschwig, J. R. Winkler, H. B. Gray, *Acc. Chem. Res.* **2009**, *42*, 1995-2004.
[9] N. Kaeffer, M. Chavarot-Kerlidou, V. Artero, *Acc. Chem. Res.* **2015**, *48*, 1286-1295.
[10] M. Razavet, V. Artero, M. Fontecave, *Inorg. Chem.* **2005**, *44*, 4786-4795.
[11] A. D. Wilson, R. H. Newell, M. J. McNevin, J. T. Muckerman, M. Rakowski DuBois, D. L. DuBois, *J. Am. Chem. Soc.* **2006**, *128*, 358-366.
[12] E. S. Wiedner, A. M. Appel, D. L. DuBois, R. M. Bullock, *Inorg. Chem.* **2013**, *52*, 14391-14403.
[13] E. S. Wiedner, J. A. S. Roberts, W. G. Dougherty, W. S. Kassel, D. L. DuBois, R. M. Bullock, *Inorg. Chem.* **2013**, *52*, 9975-9988.
[14] T. Straistari, J. Fize, S. Shova, M. Réglier, V. Artero, M. Orio, *ChemCatChem* **2017**, *9*, 2262-2268.
[15] X. Jing, P. Wu, X. Liu, L. Yang, C. He, C. Duan, *New J. Chem.* **2015**, *39*, 1051-1059.
[16] A. Z. Haddad, B. D. Garabato, P. M. Kozlowski, R. M. Buchanan, C. A. Grapperhaus, *J. Am. Chem. Soc.* **2016**, *138*, 7844-7847.
[17] A. Zarkadoulas, M. J. Field, V. Artero, C. A. Mitsopoulou, *ChemCatChem* **2017**, *9*, 2308-2317.
[18] A. Zarkadoulas, M. J. Field, C. Papatriantafyllopoulou, J. Fize, V. Artero, C. A. Mitsopoulou, *Inorg. Chem.* **2016**, *55*, 432-444.
[19] K. Ladomenou, G. Landrou, G. Charalambidis, E. Nikoloudakis, A. G. Coutsolelos, *Sustain. Energy Fuels* **2021**, *5*, 449-458.
[20] K. Ladomenou, M. Papadakis, G. Landrou, M. Giorgi, C. Drivas, S. Kennou, R. Hardré, J. Massin, A. G. Coutsolelos, M. Orio, *Eur. J. Inorg. Chem.* **2021**, *2021*, 3097-3103.
[21] M. Papadakis, A. Barrozo, T. Straistari, N. Queyriaux, A. Putri, J. Fize, M. Giorgi, M. Réglier, J. Massin, R. Hardré, M. Orio, *Dalton Trans.* **2020**, *49*, 5064-5073.
[22] T. Straistari, R. Hardré, J. Massin, M. Attolini, B. Faure, M. Giorgi, M. Réglier, M. Orio, *Eur. J. Inorg. Chem.* **2018**, *2018*, 2259-2266.
[23] R. Jain, A. A. Mamun, R. M. Buchanan, P. M. Kozlowski, C. A. Grapperhaus, *Inorg. Chem.* **2018**, *57*, 13486-13493.
[24] A. Barrozo, M. Orio, *ChemPhysChem* **2022**, *23*, e202200056.
[25] T. Straistari, R. Hardré, J. Fize, S. Shova, M. Giorgi, M. Réglier, V. Artero, M. Orio, *Chem. Eur. J.* **2018**, *24*, 8779-8786.
[26] B. C. M. Martindale, G. A. M. Hutton, C. A. Caputo, E. Reisner, *J. Am. Chem. Soc.* **2015**, *137*, 6018-6025.
[27] K. Ladomenou, G. Landrou, G. Charalambidis, E. Nikoloudakis, A. G. Coutsolelos, *Sustain. Energy Fuels* **2021**, *5*, 449-458.
[28] J. Keizer, *J. Am. Chem. Soc.* **1983**, *105*, 1494-1498.
[29] A. Barrozo, M. Orio, *RSC Advances* **2021**, *11*, 5232-5238.
[30] M. Papadakis, A. Barrozo, T. Straistari, N. Queyriaux, A. Putri, J. Fize, M. Giorgi, M. Réglier, J. Massin, R. Hardré, M. Orio, *Dalton Trans.* **2020**, *49*, 5064-5073.
[31] F. Neese, *Rev. Comput. Mol. Sci.* **2012**, *2*, 73-78.
[32] F. Neese, *Rev. Comput. Mol. Sci.* **2018**, *8*, e1327.
[33] J. P. Perdew, *Phys. Rev. B* **1986**, *33*, 8822-8824.
[34] J. P. Perdew, *Phys. Rev. B* **1986**, *34*, 7406-7406.
[35] A. D. Becke, *Phys. Rev. A* **1988**, *38*, 3098-3100.
[36] A. Schäfer, C. Huber, R. Ahlrichs, *J. Chem. Phys.* **1994**, *100*, 5829-5835.
[37] F. Neese, *J. Comput. Chem.* **2003**, *24*, 1740-1747.
[38] F. Weigend, *Phys. Chem. Chem. Phys.* **2006**, *8*, 1057-1065.
[39] V. Barone, M. Cossi, *J. Phys. Chem. A* **1998**, *102*, 1995-2001.
[40] L. Noodleman, *J. Chem. Phys.* **1981**, *74*, 5737-5743.
[41] L. Noodleman, D. A. Case, in *Adv. Inorg. Chem., Vol. 38* (Ed.: R. Cammack), Academic Press, **1992**, pp. 423-470.
[42] L. Noodleman, E. R. Davidson, *Chem. Phys.* **1986**, *109*, 131-143.

Entry for the Table of Contents

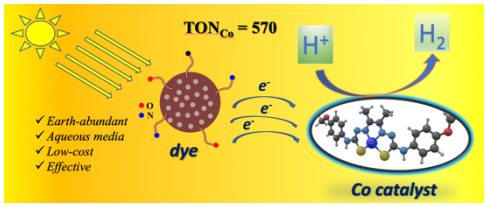

An efficient photocatalytic system with earth abundant carbon dots and a series of cobalt thiosemicarbazone catalysts was designed and studied. All prepared photocatalysts produced hydrogen reaching a rate of 358 µmol g_{NCdot}^{-1} h^{-1} upon light irradiation in water.

Institute and/or researcher Twitter usernames: @MaylisOrio, @ism2_fr